KERNFORSCHUNGSZENTRUM

KARLSRUHE

Institut für Angewandte Kernphysik

Neutron Scattering from Solid Hydrogen

W. Schott, H. Rietschel

KERNFORSCHUNGSZENTRUM KARLSRUHE

November 1970   KFK 1327

Institut für Angewandte Kernphysik

Neutron Scattering from Solid Hydrogen [+]

W. Schott, H. Rietschel
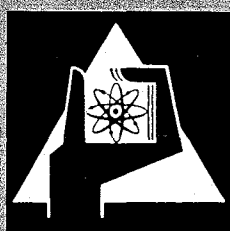
Gesellschaft für Kernforschung mbH Karlsruhe

Abstract:

By inelastic neutron scattering the quadrupole interaction constant
ratio Γ/Γ_0 in solid hydrogen has been determined to be 0.74, 0.77,
and 0.81 for ortho concentrations c = 0.68, 0.27 and 0.04, respec-
tively.
Moreover the phonon spectrum of solid hydrogen in the hcp-phase (c = 0.68)
was obtained from the scattering distribution.

Zusammenfassung:

Mit Hilfe von inelastischer Neutronenstreuung wurde die Quadrupol-
Quadrupol Wechselwirkung in festem Wasserstoff bestimmt. Für Ortho-
Konzentrationen von 68, 27 und 4 % ergab sich Γ/Γ_0 zu 0.74, 0.77
und 0.81 . Außerdem wurde die Frequenzverteilung der Phononen für festen
Wasserstoff in der hcp-Phase und der Ortho-Konzentration von 68 % aus
der Neutronenstreuverteilung erhalten.

Neutron Scattering from Solid Hydrogen

W. Schott, H. Rietschel

Kernforschungszentrum Karlsruhe

I. Indroduction

There are two groups in Western Germany working experimentally on neutron
scattering from solid hydrogen. These two groups are located at the two
research centers of Karlsruhe and Jülich. In Karlsruhe the width of the
rotational state $J = 1$ was measured in solid hydrogen by studying the
$0 \rightarrow 1$ rotational transition. Moreover, we were able to assess the frequency
distribution of the phonons from the scattering distribution by means of a
method of extrapolation. Recently we made an experiment which yields the
quadrupole coupling constant Γ at very low ortho concentration. Thereby the
splitting of the ortho molecule pairs was measured with an energy resolut-
ion of $6^o/oo$ of the $0 \rightarrow 1$ energy transfer. All the experiments were conduc-
ted at a temperature of 4.3 K, that means above the λ-point of solid hydrogen.
In Jülich, an experiment is planned at a temperature below the λ-point of
solid hydrogen. The aim of this experiment is to measure the spectrum of the
angular momentum waves.

It is known that the incoherent scattering length of the H atom is large in
relation to its coherent scattering length. The ratio of incoherent to
coherent total cross section is about 44.. Moreover, the absolute value of
the total bound cross section is relatively large, namely 81.5 barn. Condensed
hydrogen consists of ortho and para molecules with the nuclear spins of 1 and
0, respectively. The hydrogen molecules are known to rotate almost freely also
in the condensed state. The ortho molecules are in a rotational state with
$J = 1$, the para molecules with $J = 0$. Because of the symmetry of the molecule
there is a strong correlation between the nuclear spin of the molecules and
their rotational state. Scattering from the ortho molecules has an incoherent
and a coherent fraction. Scattering between the ortho- and para states is

purely incoherent, since it is coupled with a spin flip process [1,2].
The incoherent fractions accordingly result in a high intensity for these
scattering processes. Incoherent scattering can be employed to measure
frequency distributions and individual molecular excitations. The rotational
transition from $J = 0$ to $J = 1$ is an example of a molecular excitation. This
is a para-ortho transition and, hence, purely incoherent.

II. Determination of the Quadrupole Coupling Constant

II.1 Width of the rotational line

Figure 1 shows the scattering process schematically.
Neutrons with an energy of incidence E_o and a wave number vector $\vec{k}_o$ are
scattered from the sample of solid hydrogen under an angle θ. In inelastic
scattering, in which they excite a para molecule with the rotational state
of $J = 0$ into an ortho molecule with $J = 1$, the neutrons lose the energy of
the first rotational state of about 14.7 meV. Correspondingly, they leave
the sample with an energy E reduced by the rotational energy and a wave
vector $\vec{k}$. The energy transfer of 14.7 meV connected with the $0 \rightarrow 1$ transit-
ion is directly visible as a relatively sharp line in the inelastic neutron
scattering distribution.

For the intensity of the $0 \rightarrow 1$ line [3] the approximate result, if we assume
a gaussian curve with a variation of $\Delta \varepsilon$ for the shape of the line, treat
the molecules as rigid rotators, consider the spin correlation for the
scattering of neutrons from the nuclei of a molecule, and describe the
movement of the centers of mass of a molecule by a Debye Waller factor in
the Debye approximation is given by the expression:

$$(\frac{d^2\sigma}{d\Omega\, d\varepsilon})_{0 \rightarrow 1} = (1 - c) \cdot b^2_{inc} \frac{k}{k_o} \cdot 6 \cdot j^2_1 (\frac{\varkappa_{0 \rightarrow 1} \, a}{2}) \cdot e^{-\frac{3\hbar^2\varkappa^2_{0 \rightarrow 1}}{4M\Theta_D}} \cdot \frac{e^{-\frac{(\varepsilon - E_{J=1})^2}{2\Delta\varepsilon^2}}}{\sqrt{2\pi\Delta\varepsilon^2}}$$

In this formula, c is the ortho concentration, b_{inc} the bound incoherent scattering length, k_o and k are the wave numbers of the incident and scattered neutrons, respectively, j_1 is a spherical Bessel function, $\hbar\varkappa_{o \to 1}$ is the momentum transfer of the scattered neutrons, M the mass of the molecule, Θ_D the Debye temperature.

The width of this line is given essentially by the resolution of the equipment, which is known [4], and the quadrupole quadrupole interaction between the ortho molecules. Hence, an exact knowledge of the physical line width allows conclusions with respect to the quadrupole coupling parameter Γ.

Figure 2 shows the rotating crystal time-of-flight spectrometer we used to measure the inelastic scattered neutrons.
Neutrons of a thermal beam are reflected from the 111 planes of a rotating Al crystal. On the basis of Bragg's equation $n\lambda = 2d \sin \Theta$, specific wavelengths and energies, respectively of the n order correspond to each scattering angle 2Θ. These monochromatic neutrons are impinging upon the sample of solid hydrogen contained in a helium crystat set up at the place of the sample (the cryostat is not shown in the picture). The cryostat cools the hydrogen sample with cold helium gas which is maintained at a temperature of 4.3 K. The neutrons scattered from the sample can be registered by a maximum of nine detectors. Since the crystal rotates, Bragg's condition is fulfilled only during a short interval of time. Therefor, two short neutron bursts are produced at each rotation. The energies of the scattered neutrons are determined from the measurement of the time-of-flight they require to cover the distance between the sample and the detector. The starting pulse is generated by a magnetic trigger attached to the rotating crystal.

Figure 3 shows two time-of-flight spectra measured with this system. The spectra were measured at 4.3 K and two different ortho concentrations of 68 and 27 %. The $0 \to 1$ and the $1 \to 0$ transitions are visible, and so is the elastic line and a broad spectrum which is due to the excitation of single and multi phonon processes. An enlargement of the line width of the $0 \to 1$ peak at the higher ortho concentration is clearly recognizable. The phonon spectrum will be discussed later. The peaks were evaluated by a least squares

fit of a gaussian distribution. For c = 0.68 the background due to multi phonon processes was described by an exponential function. For c = 0.27 the background can be represented approximately by a straight line, due to the lower intensity of multi phonon scattering which is caused by the scattering from ortho molecules.

Figure 4 shows the 0 → 1 line at 27 % ortho concentration. The fit with a gaussian distribution can be carried out very well. The two curves correspond to two different scattering angles. The dashed line corresponds to the unfolded curve where the resolution of the equipment has been folded out.

Figure 5 shows the 0 → 1 line at 68 % ortho concentration. One example of a spectrum with background and three examples of different scattering angles with the background subtracted are pictured. Obviously, at this high ortho concentration the line can not be described in a satisfying way by a gaussian curve. Instead, there is a structure, which may have however no major influence upon the line width. One possible explanation is that even above the λ-point collective modes of the angular momentum waves still exist. A spectrum which is similar to the angular momentum wave spectrum would explain the structure of the rotational line. Furthermore the steep descent of the line to higher energies is then due to the fact that angular momentum waves which have an energy of about 12 K are not excited at 4.3 K.

Elliott and Hartmann [5] carried out a theoretical treatment of neutron scattering from condensed hydrogen. They based their argument on the assumption that the ortho molecules are unoriented. Thus, the theory holds for temperatures above the λ-point. Moreover, they considered only the interaction between two ortho molecules and they used in the perturbation theory the nine possible wave functions of state of a pair of free ortho molecules. For the mean square of the energy transfer of the 0 → 1 rotational transition their result is then as follows:

$$\overline{\Delta\varepsilon^2} = c \cdot \frac{70}{9} \cdot \Gamma^2 \cdot \sum_{j(\neq i)} \left(\frac{R_0}{R}\right)^{10}$$

Here, $\Gamma_o = \frac{6}{25} \frac{Q^2}{R_o^5}$ is the quadrupole coupling parameter. Q is the quadrupole moment of the H_2 molecule, and R_o is the distance of the nearest neighbors of the molecules in the hcp lattice. The root of the mean square energy transfer $\sqrt{\overline{\Delta\epsilon^2}}$ is connected with the full line width at half height of a gaussian curve $\Delta E_{0 \to 1}$ by

$$\Delta E_{0 \to 1} = 2.358 \cdot \sqrt{\overline{\Delta\epsilon^2}_{0 \to 1}}$$

In this model only the electric quadrupole quadrupole (EQQ) interaction was considered. Van der Waals and valence forces, which also have a contribution that is effective between the ortho molecules, have an effect of only about 2 % relative to the quadrupole forces. We used the formula by Elliott and Hartmann to calculate Γ from our measured line width.

For the sum $\sum\limits_{j(\neq i)} \left(\frac{R_o}{R}\right)^{10}$ the value of 12.312 results for the hcp lattice according

to Wallace and Patrick [6]. The table (Fig. 6) shows the line widths of the rotational lines $\Delta E_{0 \to 1}$ measured at the ortho concentration c and momentum transfer $\hbar\varkappa$. The width ΔE_{App} caused by the finite resolution of the equipment was calculated. The line widths do not depend on $\varkappa$. From $\overline{\Delta E_{0 \to 1}}$, an average over the measurements with different $\varkappa$, and the same ortho concentration, we obtained Γ. The ratio Γ/Γ_o is below unity, where Γ_o is calculated simply by using the above formula with $R_o = 3.755$ Å. For Γ_o we used a value of 0.0866 meV given by A.B. Harris [7]. For Γ/Γ_o at an ortho concentration c = 0.27 a value of 0.77 results, for c = 0.68 a value of 0.74 .

II.2 Measurement of the Ortho Pair Spectrum Levels

Figure 7 shows the principle arrangement of our neutron scattering experiment aiming for a high energy resolution to measure the splitting of the ortho molecule pairs directly if the contribution of the higher ortho molecule clusters can be neglected. Therefore we chose a sample containing only 4 % ortho hydrogen. The probability that an ortho molecule is surrounded only by para molecules is in this case 61 % and the probability for just one ortho

molecule neighbour is 23 %. The temperature of the sample was 4.4 K. We used a pseudostatistical chopper [8] which enables one to measure the scattered distributions like in a conventional time-of-flight experiment if one cross correlates the scattered neutron distribution with the special pattern of the chopper. The chopper consists of a disk with an arrangement of slits. With this pattern the disk is half of the time transparent and half of the time black for neutrons. Therefor a factor of roughly 50 in intensity can be gained in comparison with a rotating crystal. In our case we gained only a factor of 6.8 because the peaks to be measured were about of the same height as the mean value of the time-of-flight spectrum. The cross correlating will be done by a computer. We used a copper single crystal as a monochromator. After the sample there is a flight path of 9 m. For the 0 → 1 transition we achieved in this way an energy resolution of about $6^{\circ}/oo$. The energy of the incident neutrons is $E_o = 19.26$ meV.

Figure 8 shows a photograph of this arrangement. The direct beam, the cryostat and the flight path can be seen.

If we take only the EQQ interaction between the ortho molecule pairs into account we expect a 4 level scheme [9] in which the splitting is given by -4Γ (2), 0 (4), Γ(2), 6Γ (1) (the numbers in parentheses denote the degeneracy). This splitting should be seen in the scattered distribution.

Figure 9 shows the folded spectrum which corresponds to a conventional time-of-flight spectrum. The main peak originates from an excitation of a para molecule into an ortho molecule which is surrounded only by para molecules. This peak is broadened because of three reasons:

(a) The width of the resolution function of the spectrometer for the rotational line was calculated to be about 100 μeV corresponding to an energy resolution of $6^{\circ}/oo$ for the 0 → 1 energy transfer.

(b) The EQQ interaction between ortho molecules with mutual distances larger than the nearest neighbour distance. This effect causes a broadening of 51 μeV $\underline{/5\underline{7}}$.

(c) The line E_o - 14.79 $-\Gamma$ = (4.47 $-\Gamma$) meV which is broadened by a) and b) is included in the peak.

   Furthermore the main peak contains the unsplit level of the ortho

molecule pair spectrum at E_o - 14.79 = 4.47 meV.

The **other** two lines of the pair spectrum corresponding to a splitting
of +6Γ and -4Γ can be seen as weak lines on both sides of the main
peak. Especially the last one is certainly out of statistics. The ordinate
shows the counts which are to be expected with a conventional rotating
crystal chopper. Because of the pseudostatistical technique the absolute
error is about 1/2 $\sqrt{counts}$. The expected spectrum was fitted to the
measured points. This spectrum has been calculated by superposing gaussian
lines corresponding to the contribution of soloists and pairs. The con-
tribution of higher ortho molecule clusters was approximated by a gaussian
distribution by means of the theory of Elliott et al. $\underline{/5\_7}$. The width of
this distribution turned out to be 7 times as large as the width of the
soloist- and pair lines. Thus, the higher ortho clusters produce only a
flat background which hardly effects the spectrum. Γ and the width of the
soloist- and pair lines W were used as parameters for the least squares fit
and determined to be Γ = (70.0 $\pm$ 0.03) μeV and W = 112 μeV. This yields
Γ/Γ_o = 0.81 $\pm$ 0.03 which is in very good agreement with NMR experiments
$\underline{/11\_7}$.

Our experimental results show that Γ/Γ_o is larger for low concentration
or dilute ortho hydrogen than for concentrated ortho hydrogen. In both cases
the value is smaller than one. This result is supported by calculations of
A.B. Harris $\underline{/12\_7}$. Γ is changed in the crystal by the interaction of
phonons with orientational states and by dielectric screening. The interaction
with the phonons can be divided into a static and a dynamic part. Whereas
the static part is the same for concentrated and dilute ortho hydrogen and
leads to a reduction of Γ , the dynamic part is different for both cases
and causes Γ to decrease and increase for concentrated and dilute ortho
hydrogen, respectively. The dielectric screening leads to an effective de-
crease of the EQQ interaction by about the same amount in both cases. The
dielectric screening which is caused by three body interactions also changes
the separations of the EQQ pair levels relatively to each other. In fact it
is rather difficult to observe theses relative shifts of the EQQ pair levels.
Taking three body interactions into account, the 6Γ peak, for example, is
expected to be shifted by about 0.02 Γ_o to lower energies if the remaining
part of the spectrum is fitted by a superposition of gaussian functions accor-

- 8 -

ding to the contributions of soloists and ortho molecule pairs (EQQ spectrum) as we have done.

III. Phonon frequency distribution of concentrated ortho hydrogen in the hcp phase

Besides the O → 1 transition, the incoherent neutron scattering distribution yields the phonon spectrum as another item of information. The differential cross section for neutron scattering from a system of identical nuclei with a statistical orientation of the nuclear spin can be written as

$$\frac{d^2\sigma}{d\Omega\, d\mathcal{E}} = \frac{\sigma_b}{4\pi\, k_B \cdot T} \cdot \frac{k}{k_o} \cdot e^{-\frac{\beta}{2}} \cdot s(\alpha,\beta)$$

where σ_b means the bound total cross section.

$$\beta = \frac{E - E_o}{k_B \cdot T} = -\frac{\mathcal{E}}{k_B \cdot T}$$

is proportional to the energy transfer and

$$\alpha = \frac{\hbar^2 |\vec{k}_o - \vec{k}|^2}{2Mk_B \cdot T} = \frac{\hbar^2 \varkappa^2}{2Mk_B \cdot T}$$

is proportional to the square of the momentum transfer.

S (α,β) is the scattering law. This formula applies also to the scattering from phonons in solid hydrogen in the incoherent approximation where the scattering law S reduces to the self term S_s, i.e., where coherent scattering may be neglected. Only the ortho molecules contribute to the scattering law S_s for the excitation of phonons, because the scattering in the para state is coherent and negligeable. It has been shown by Egelstaff et al. [13] that the phonon spectrum g ($|\mathcal{E}|$) can be obtained from S_s by means of a method of extrapolation. The procedure may be described by the following relation:

$$\left(\frac{S_s}{\alpha}\right)_{\alpha \to 0} = \frac{\mathscr{P}(\beta)}{2\beta \sinh \beta/2} = \frac{k_B \cdot T \cdot \rho(|\mathcal{E}|)}{2\beta \cdot \sinh \beta/2}$$

The $\mathscr{P}(|\mathcal{E}|)$ obtained in each case has the character of a frequency spectrum. In the case of a harmonic solid this relation follows from the phonon expansion.

Figure 10 shows a plot of S_s/α as a function of α on a logarithmic scale. The measured points then should be roughly on a straight line because of the Debye Waller factor, which has the form of $e^{-\lambda \alpha}$. From the slope an average of the Debye Waller coefficient λ can be calculated. The points up to $\alpha \approx 60$ are very well arranged on a straight line. At small β-values, the resulting S_s/α -values are too high because of the finite width of the elastic line, mainly due to the resolution of the equipment. Correspondingly, the extrapolation and the resulting frequency distribution are relatively inaccurate at small β-values. The solid lines represent an attempt to reconstruct the scattering law S_s by means of the phonon spectrum obtained via a phonon expansion. Moreover, we averaged over the polarization vectors of the phonons, which is correct only for cubic crystals [14]. Nevertheless, the values of S are quite reasonable. For a hcp lattice the Debye Waller factor is anisotropic. Correspondingly, we obtained a Debye Waller factor averaged over the polarzation vectors of the phonons. The root of the mean square shift of the molecules of 0.588 Å calculated in this way is in good agreement with the value of 0.6 Å obtained by Mertens and Biem [15] for fcc para-hydrogen. Furthermore the value $\Theta = 109.5$ K (at T = 4.3 K) obtained for the Debye temperature is reasonable. From sonic velocities [16] a value of Θ (T = 0) = 115 K was deduced.

Figure 11 shows the extrapolated phonon spectrum for solid hydrogen with c = 0.68 and T = 4.3 K. For comparison, we have included the phonon spectrum by Mertens and Biem for hcp para hydrogen. This calculation was carried up to neighbours of the second order.
Both spectra agree in the number and the relative position of the peaks. The

width of the calculated spectrum is smaller than the measured one. This
discrepancy may vanish by inclusion of neighbours of higher order in the
calculation. The width of the theoretical spectrum was found to be 8.1 meV
with one shell and 9.4 meV with two shells of neighbours. Another discrepancy
is the last peak.
There may be no difference between ortho- and para hydrogen in the spectrum
of the lattice vibrations above the λ-point. The quadrupole quadrupole forces
may cancel each other, because the molecules are not very much orientated.

Figure 12 shows the dispersion curves for hcp para hydrogen by Mertens and
Biem. The calculation has carried out in the Random Phase Approximation.

Figure 13 shows the specific heat calculated from our extrapolated phonon
spectrum. For comparison, we have included the experimental C_v (T) values
by Ahlers [17]. These measurements were carried out on para hydrogen. The
values by Ahlers were converted to a molar volume corresponding to our
measurement of 22.68 cm^3/mol. The values calculated from the frequency
distribution are higher than the experimental ones over the entire range of
temperature. This deviation may be due to insufficient knowledge of the fre-
quency distribution at low energy transfer. However, the experimental values
by Ahlers result in a very high Debye temperature of Θ (T = 0) = 127 K.

References
_____

/ 1 _/ Young, J.A. and J. U. Koppel, Phys. Rev. 135, A 603, 1964

/ 2 _/ Sarma, Q., Proceedings of the International Atomic Energy
        Agency Symposium on Inelastic Scattering of Neutrons in
        Liquids and Solids, Vienna, 1960 (International Atimic
        Energy Agency, 1961)

/ 3 _/ Egelstaff, P., B. Haywood and F. Webb, Proc. Phys. Soc.,
        90, 681-96, 1967

/ 4 _/ Carvalho, F., G. Ehret, W. Gläser, Nucl. Instr. and Meth.
        49 (1967), 197-216

/ 5 _/ Elliott, R.J. and W.M. Hartmann, Proc. Phys. Soc., 90,
        671-80, 1967

/ 6 _/ Wallace D.C. and J.L. Patrick, Phys. Rev., 137, A 152, 1965

/ 7 _/ Harris, A.B., Int. Journ. Quantum Chem., IIS, 347 (1968)

/ 8 _/ Gompf, F., W. Reichardt, W. Gläser and K.H. Beckurts, Pro-
        ceedings of the International Atomic Energy Agency Symposium
        on Neutron Inelastic Scattering, Copenhagen, 1968

/ 9 _/ Sears, V. and J. van Kranendonk, Canad. J. Phys. 42, 980-1103,
        1964

/ 10 _/ Hardy, W. and J.R. Gaines, Phys. Rev. Letters 19, 1417 (1967)

/ 11 _/ Harris, A.B., L.I. Amstutz, H. Meyer and S.M. Myers, Phys.
        Rev. 175, 603 (1968)

/ 12 _/ Harris, A.B. Phys. Rev. 1, B 1881 (1970)

/ 13 _/ Egelstaff, P.A., P. Schofield, Nucl. Sci. Eng. 12, 260 (1962)

/ 14 _/ McLatchie, P., LEAP Programm Description, AERE Harwell (1962)

/ 15 _/ Mertens, F.G. and W. Biem, private communication

/ 16 _/ Bezuglyi, P.A. and R. Kh. Minyafaev, Sov. Phys. Solid State
        9, 480, 1967

/ 17 _/ Ahlers, G., J. Chem. Phys. 41, 86 (1964)

Figure captions
_____

Fig. 1   Scattering process, schematically

Fig. 2   Rotating crystal time-of-flight spectrometer at the FR2

Fig. 3   Time-of-flight spectra E_o = 21.75 meV, c = 0.68, ϑ = 55.2

Fig. 4   0 → 1 Rotational lines c = 0.27

Fig. 5   0 → 1 Rotational lines c = 0.68

Fig. 6   Table

Fig. 7   Experimental arrangement with high energy resolution

Fig. 8   Photograph of the high resolution arrangement

Fig. 9   Ortho molecule pair spectrum

Fig. 10 $S(\alpha,\beta)/\alpha$ of solid hydrogen c = 0.68

Fig. 11 Phonon spectrum of solid hydrogen c = 0.68

Fig. 12 Phonon dispersion curves of para hydrogen in the hcp phase

Fig. 13 Specific heat of solid hydrogen c = 0.68

0→1 Rotational Line

ΔE

$(E_o - 14{,}7\,meV)$

H_2-sample

Θ

$\vec{k}_o, E_o$

$\vec{k}, E = E_o - 14{,}7\,meV$
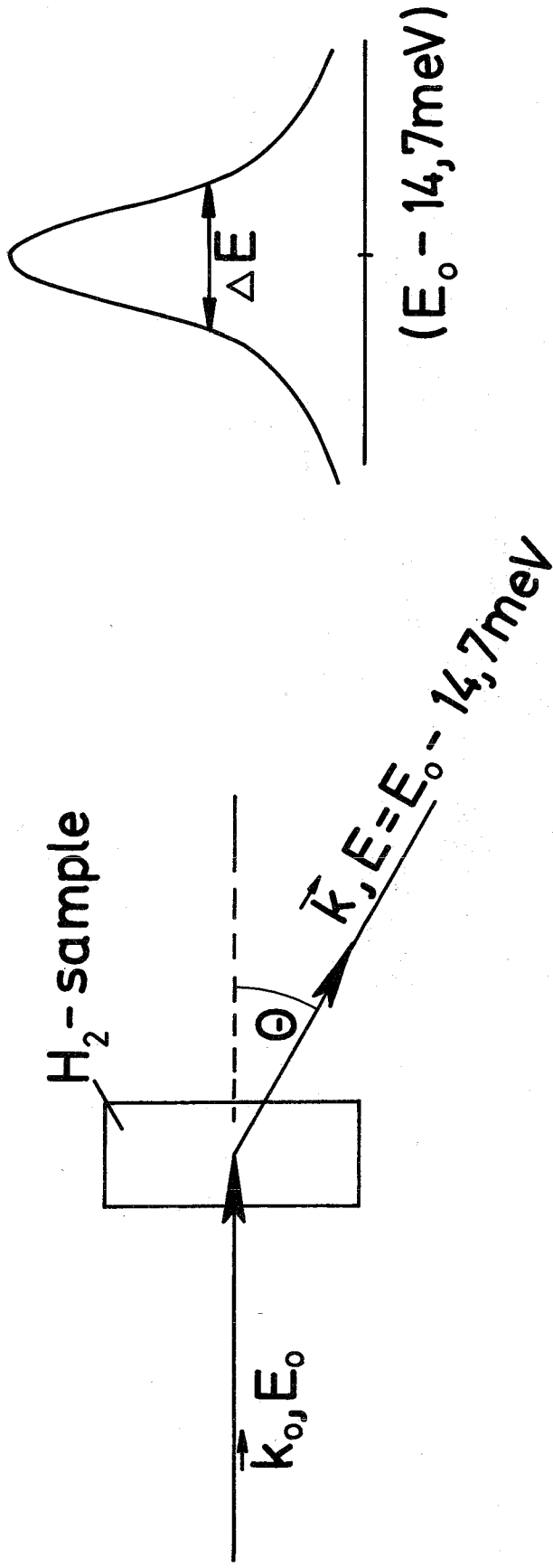
$$\left(\frac{d^2\sigma}{d\Omega\,d\varepsilon}\right)_{0\to1} = (1-c)\cdot b_{inc.}^2 \cdot \frac{k}{k_o} \cdot 6\,j_1^2\!\left(\frac{\varkappa_{0\to1}\cdot a}{2}\right) e^{-\frac{3\hbar^2\,\varkappa_{0\to1}^2}{4M\Theta_D}} \cdot \frac{e^{-\frac{(\varepsilon - E_{J=1})^2}{2\,\Delta\varepsilon^2}}}{\sqrt{2\pi\,\Delta\varepsilon^2}}$$

Fig. 1

Rotating crystal time-of-flight spectrometer at the FR 2

Fig. 2

a)

b)

Counts

9000
7000
5000
3000

5000
4000
3000
2000

0→1

1→0

0→1

1→0

Channelnumber

100   120   140   160   180   200   220
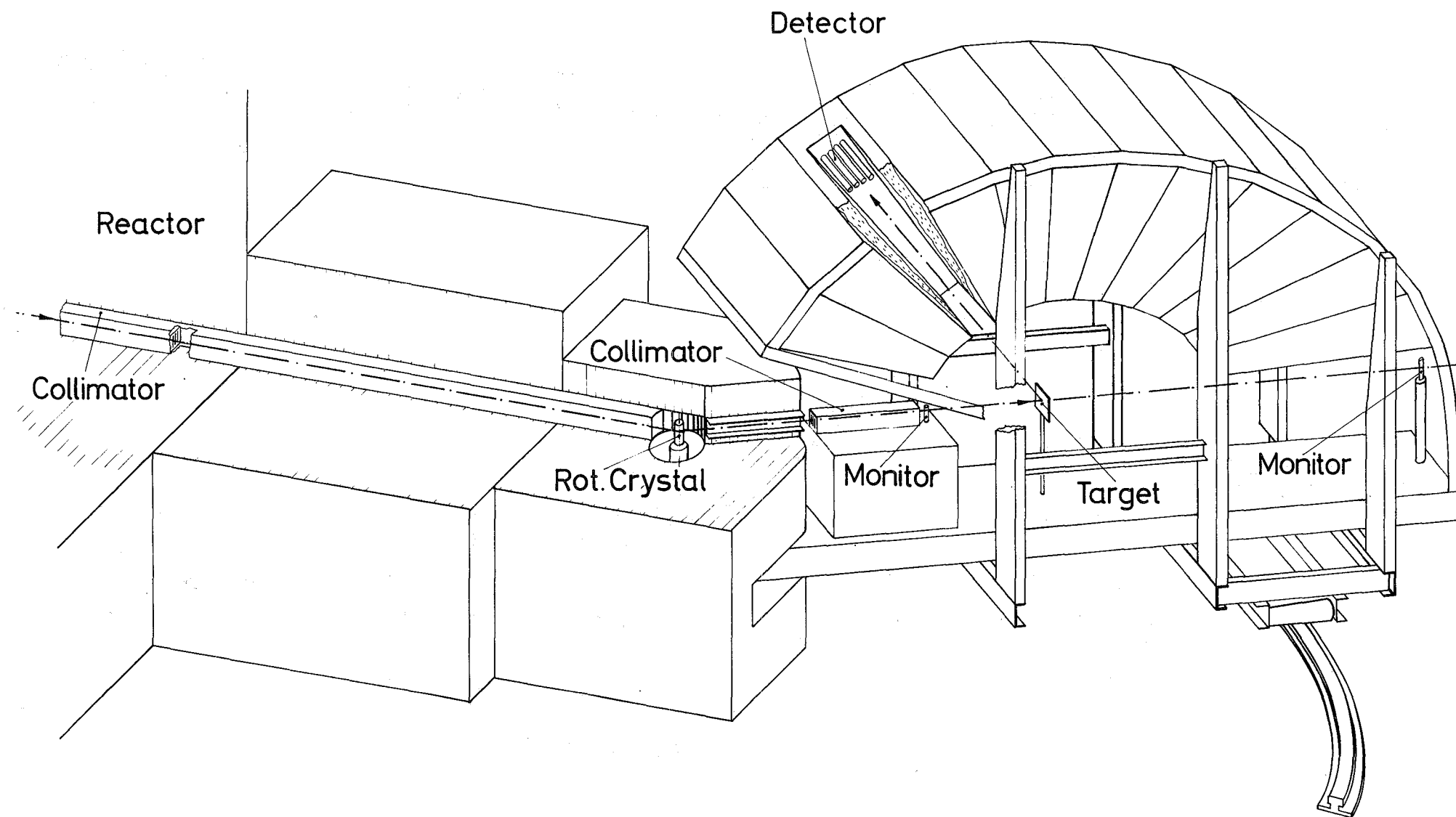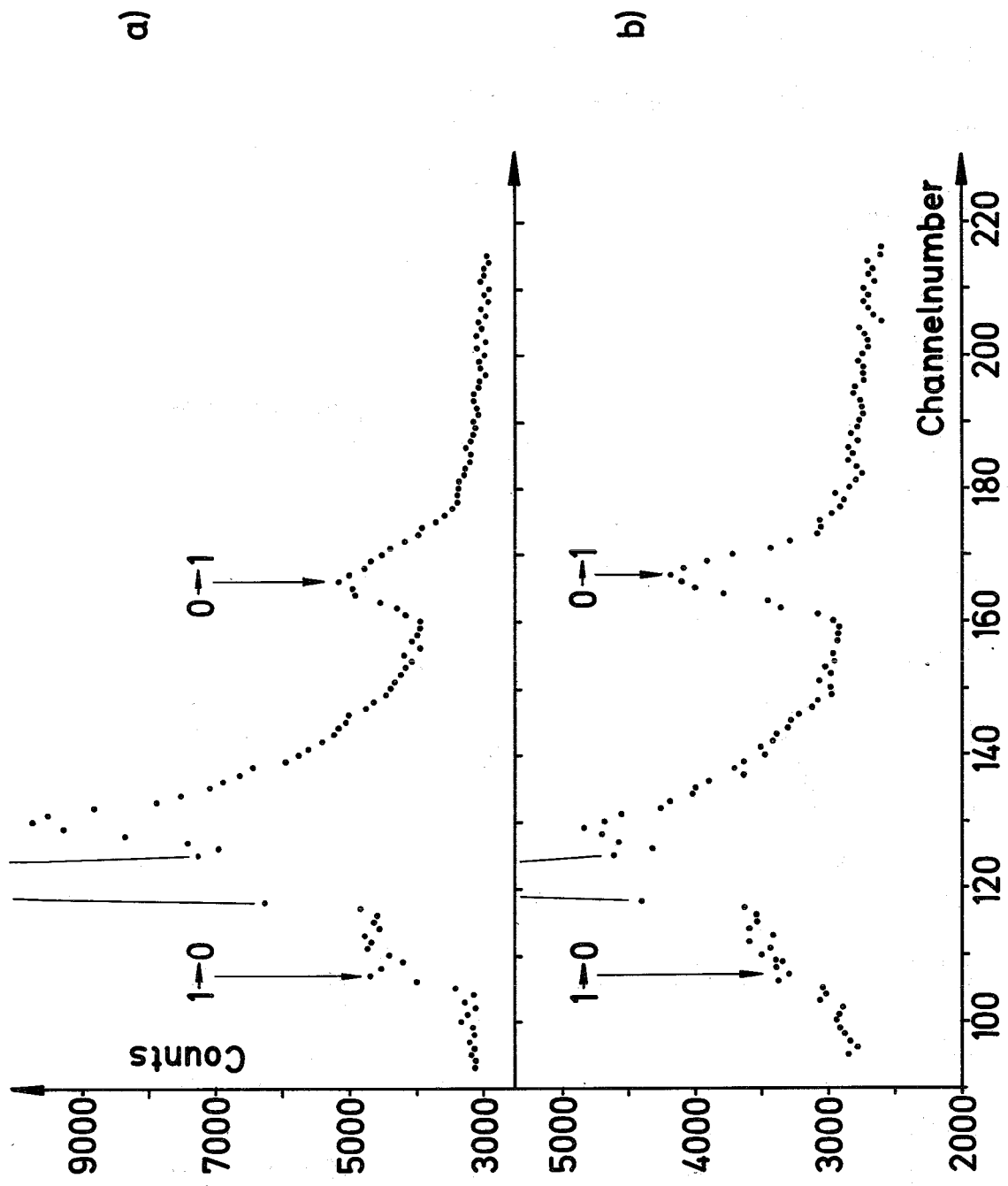
Time of Flight Spectra $E_0 = 21.75$ meV; $T = 4.3°K$; $c = 0.68$;
$\vartheta = 55.2°$

Fig. 3
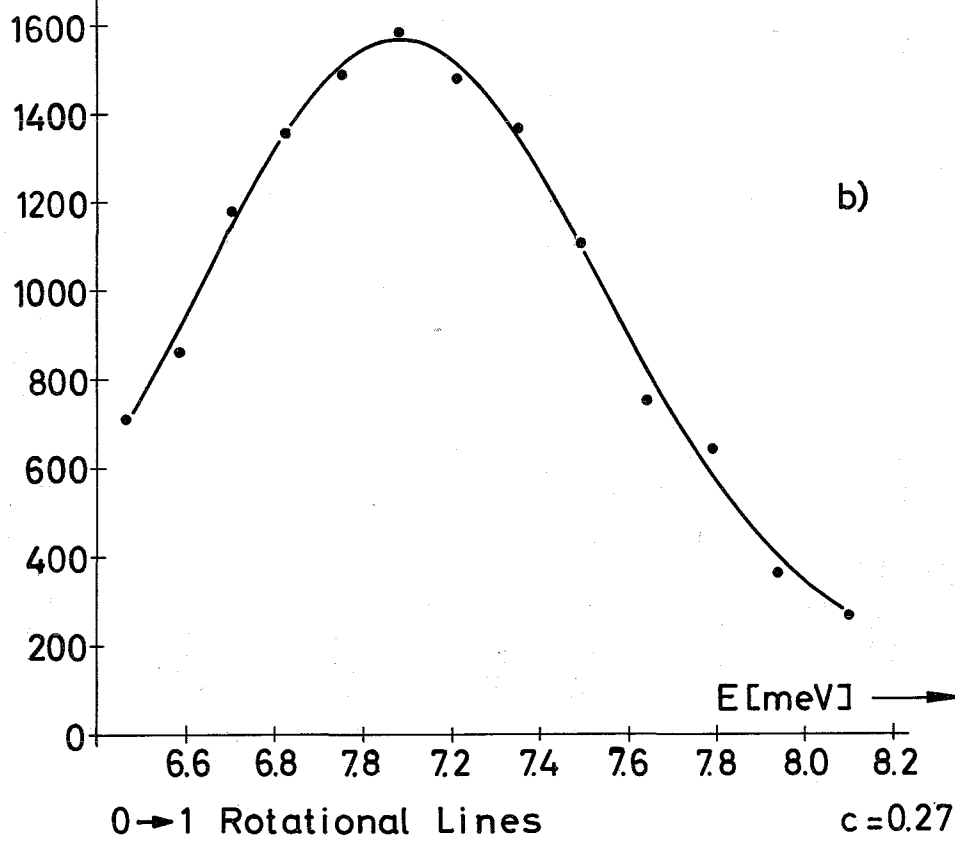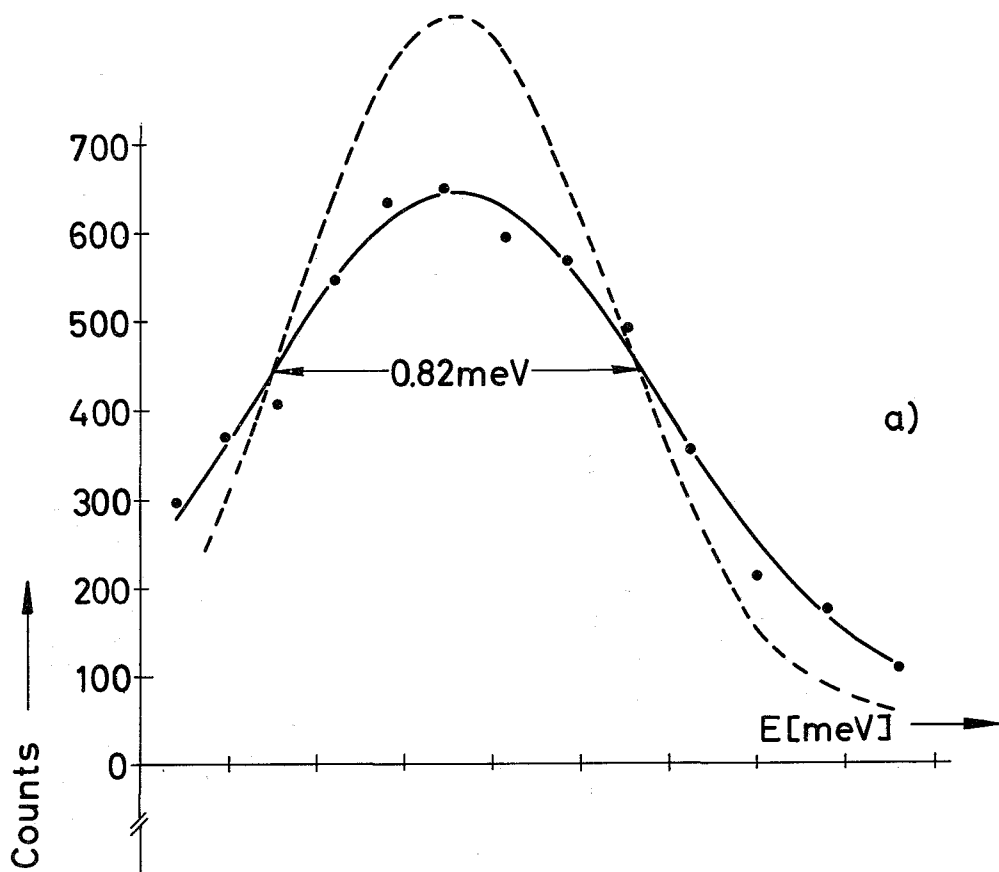
Fig.4
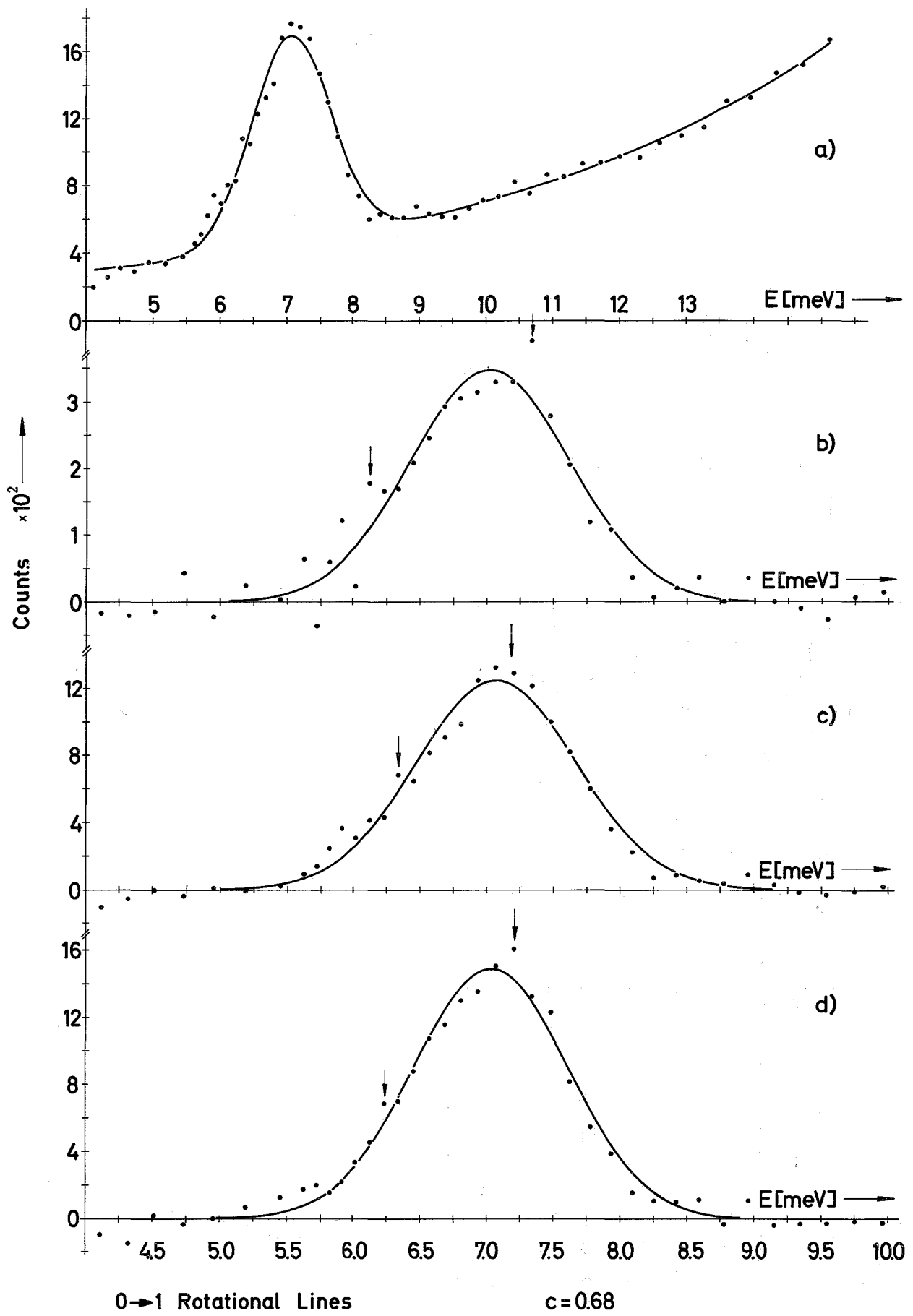
Fig. 5

Table

c	$\kappa^2 [\text{Å}^{-2}]$	$\Delta E_{App} [\text{meV}]$	$\Theta [°]$	$\Delta E_{0\to1} [\text{meV}]$	$\overline{\Delta E_{0\to1}} [\text{meV}]$	Γ	$\dfrac{\Gamma}{\Gamma_o}$
0.27	5.28	0.71	43.9	0.82 ± 0.07			
0.27	7.07	0.71	55.2	0.79 ± 0.07	0.80	0.0667	0.77
0.68	3.82	0.66	32.5	1.24 ± 0.07			
0.68	5.28	0.66	43.9	1.23 ± 0.07	1.22	0.0641	0.74
0.68	7.07	0.67	55.2	1.18 ± 0.07			

Γ_o = 0.0866 meV

Fig.6

detector

$E_0 - 14.7\,\text{meV}$

Reactor

statistical
chopper

H_2

E_0

direct beam

Cu-
-monochromator
[311]-planes

Experimental arrangement with
high energy resolution.
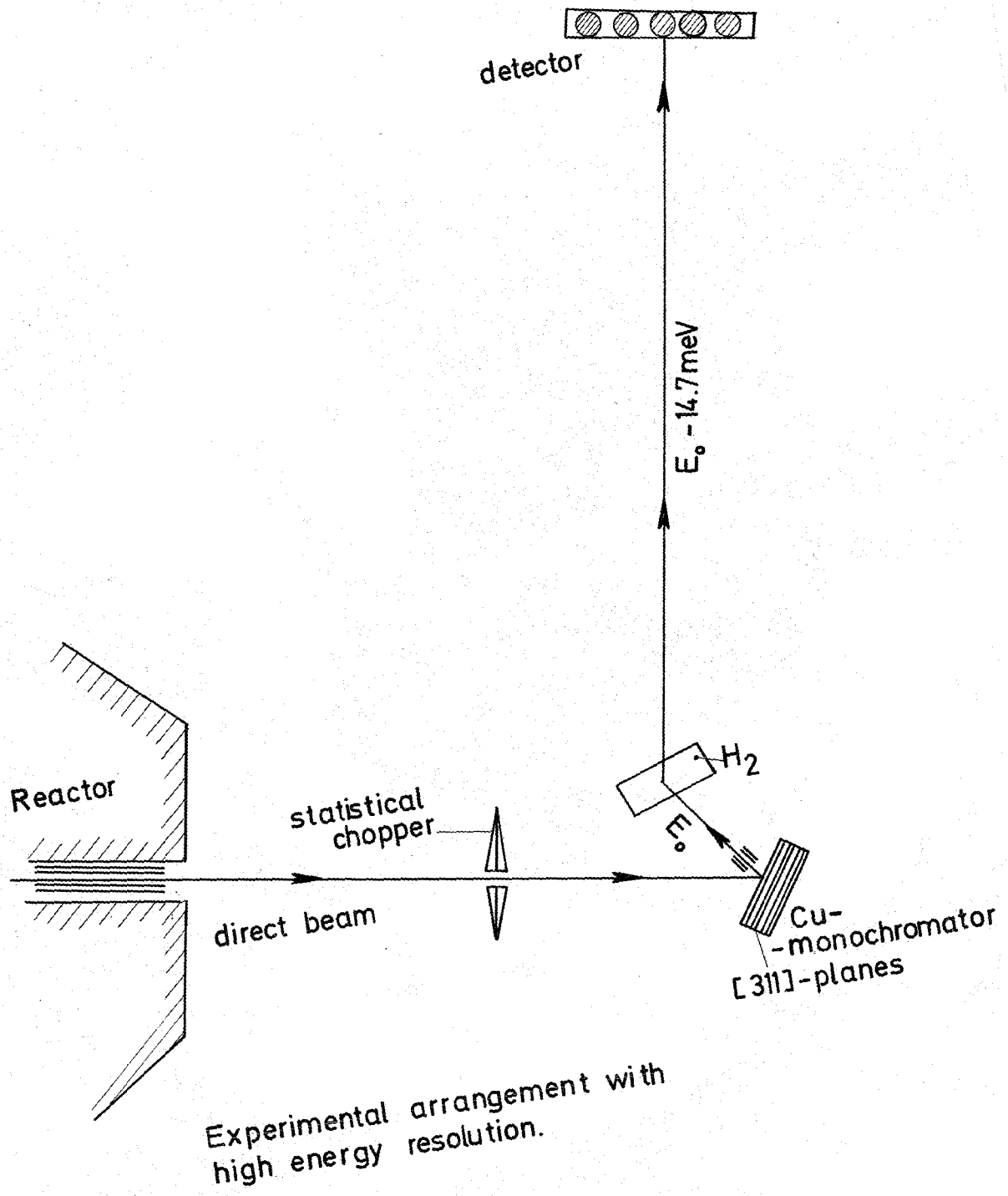
Fig.7
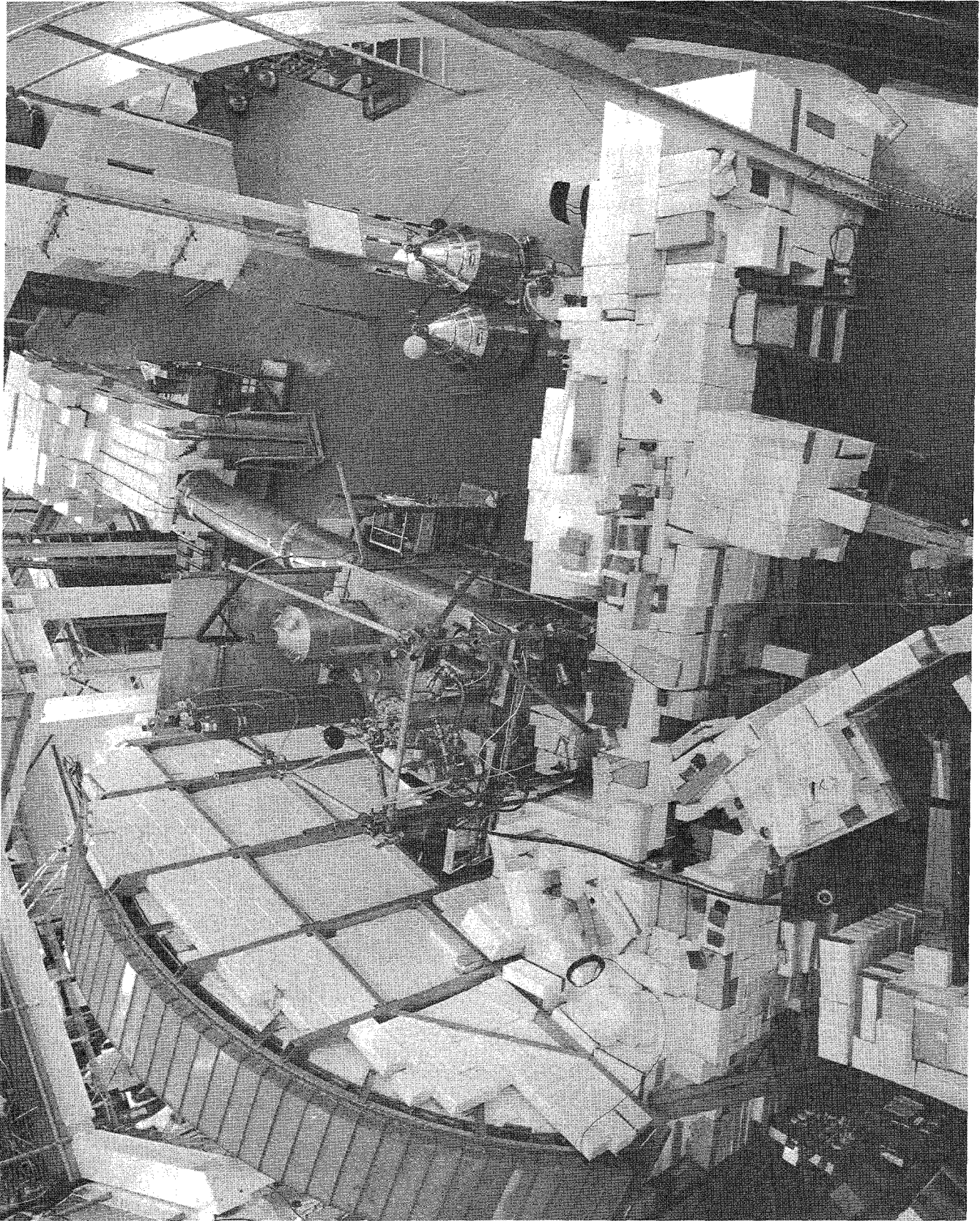
Fig. 8
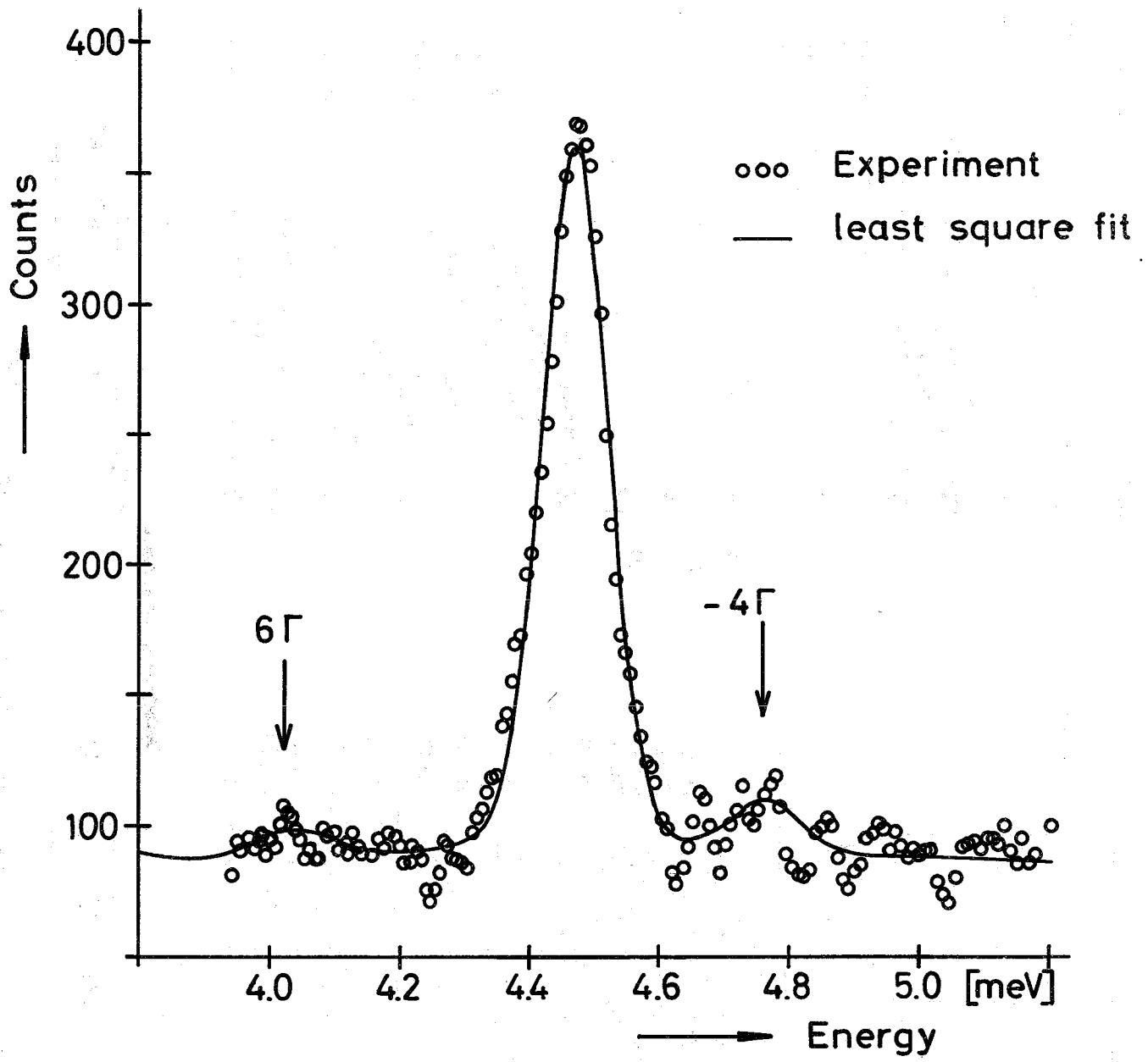
Fig.9
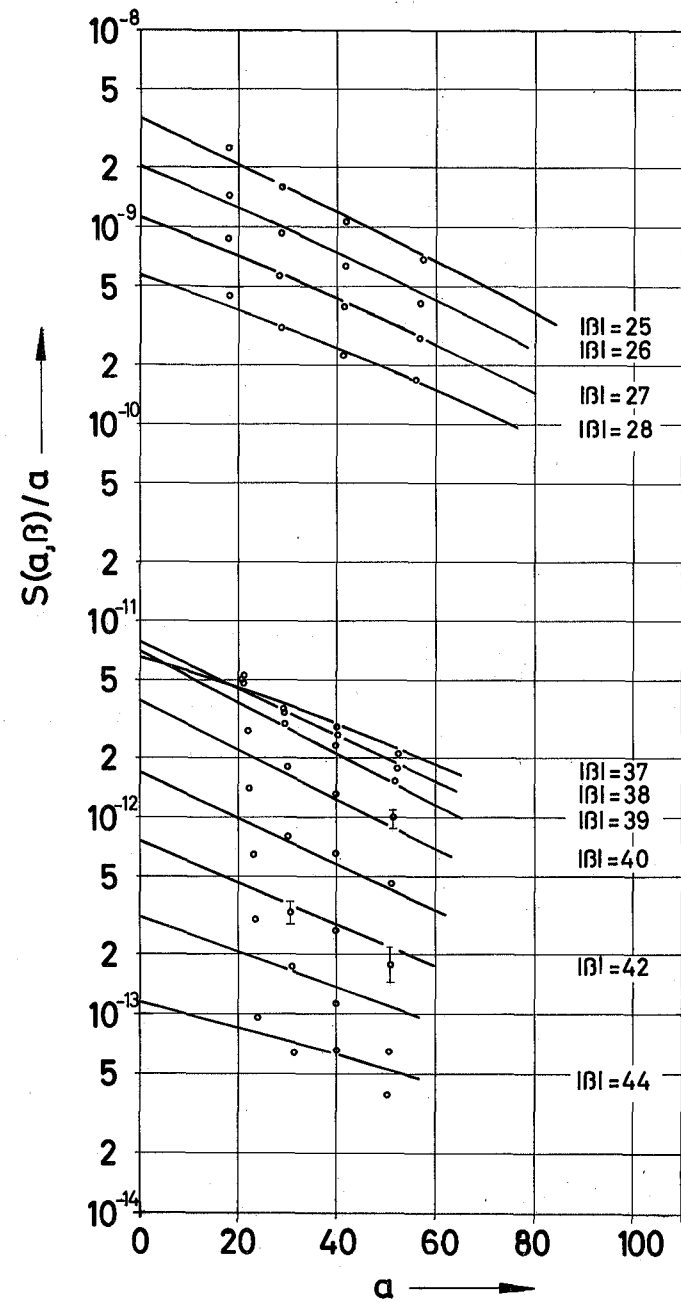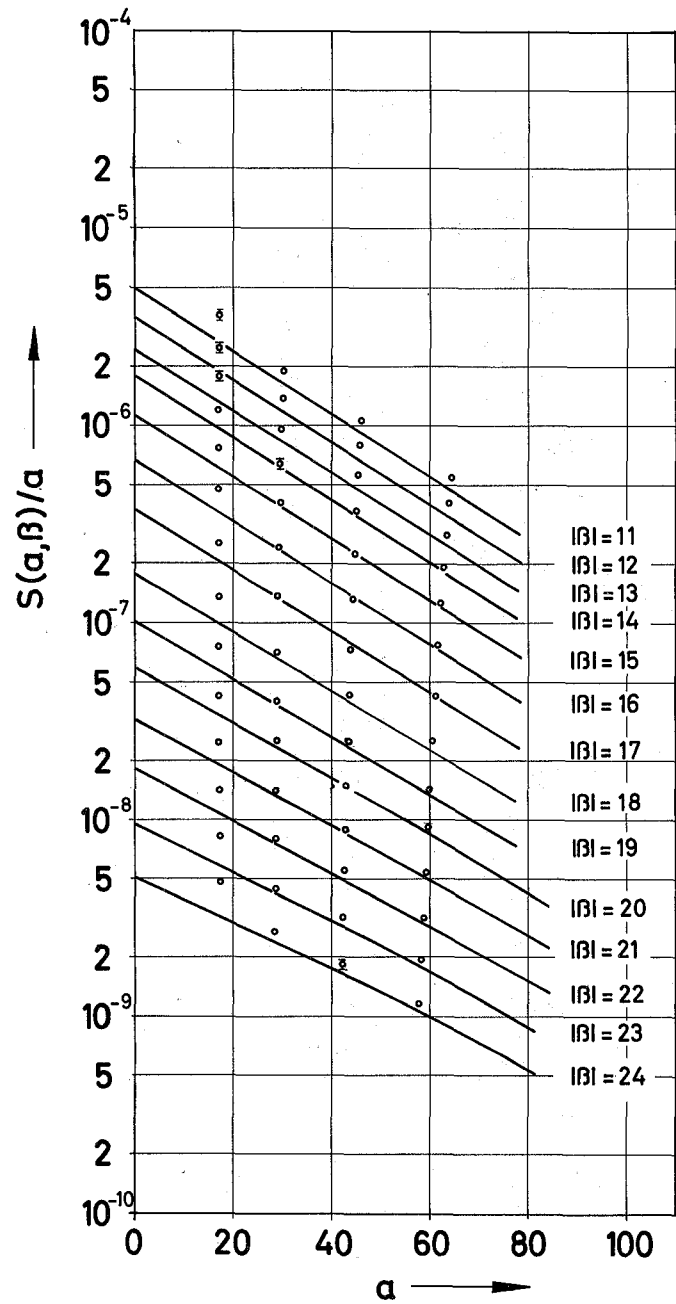
S(α,β) / a   of Solid Hydrogen , c = 0.68; T= 4.3°K

Fig.10
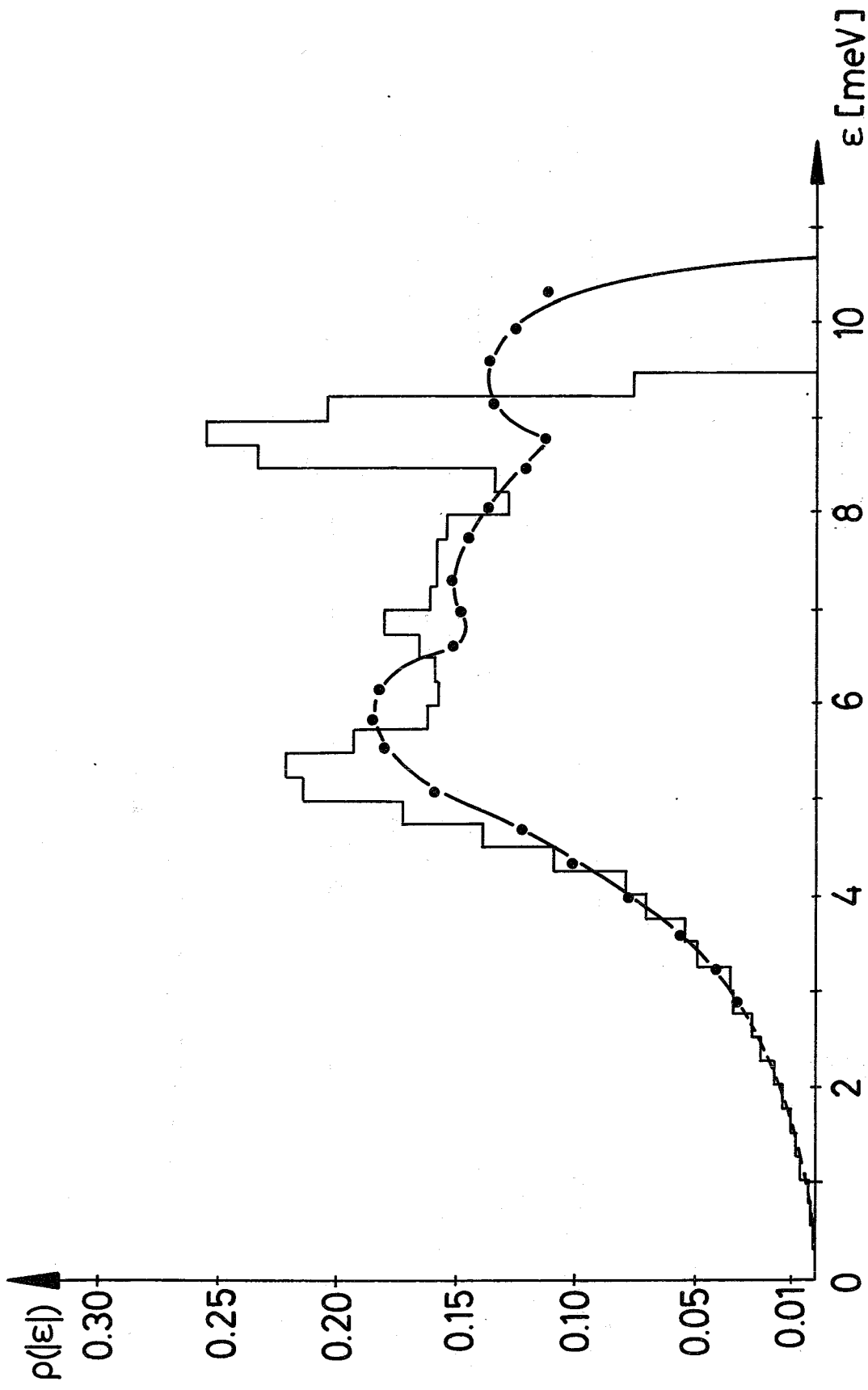
Phononspectrum of Solid Hydrogen. c=0.68   T = 4.3 °K

Fig.11
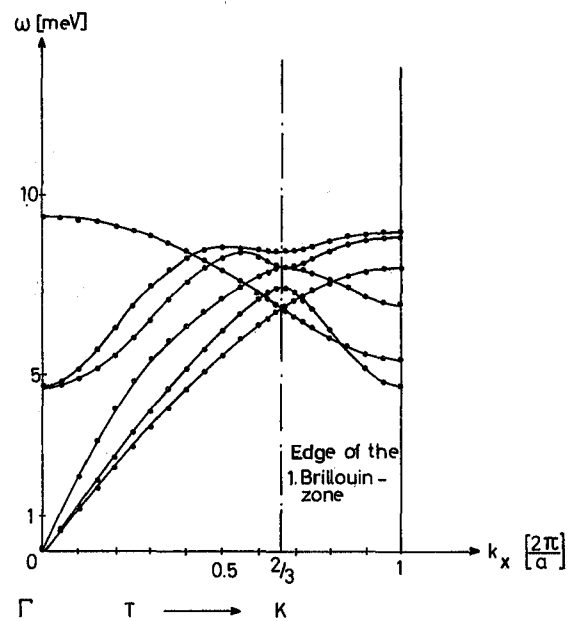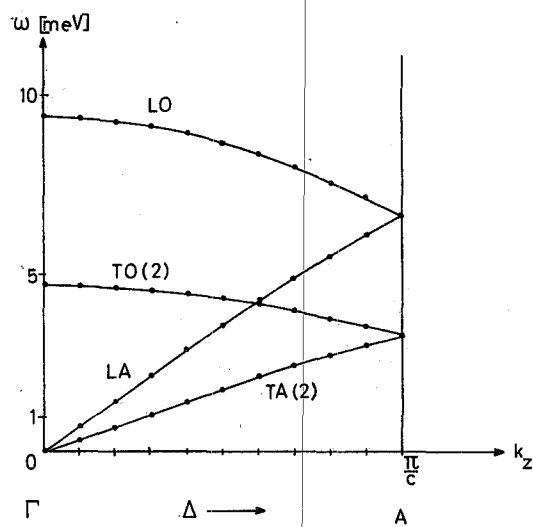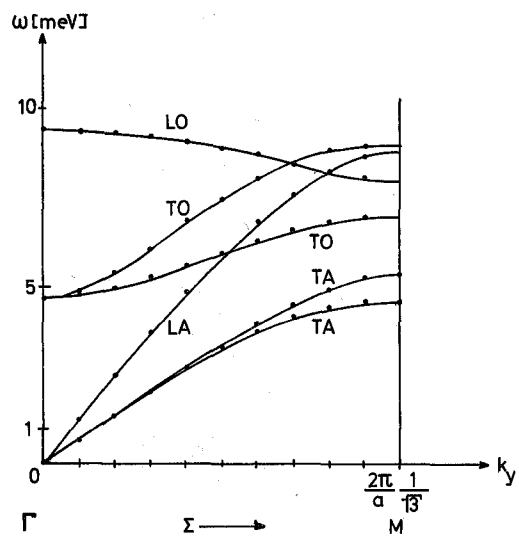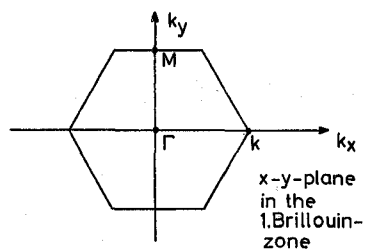
PHONON-DISPERSION CURVES OF PARA – H$_2$ (HCP)

Fig.12
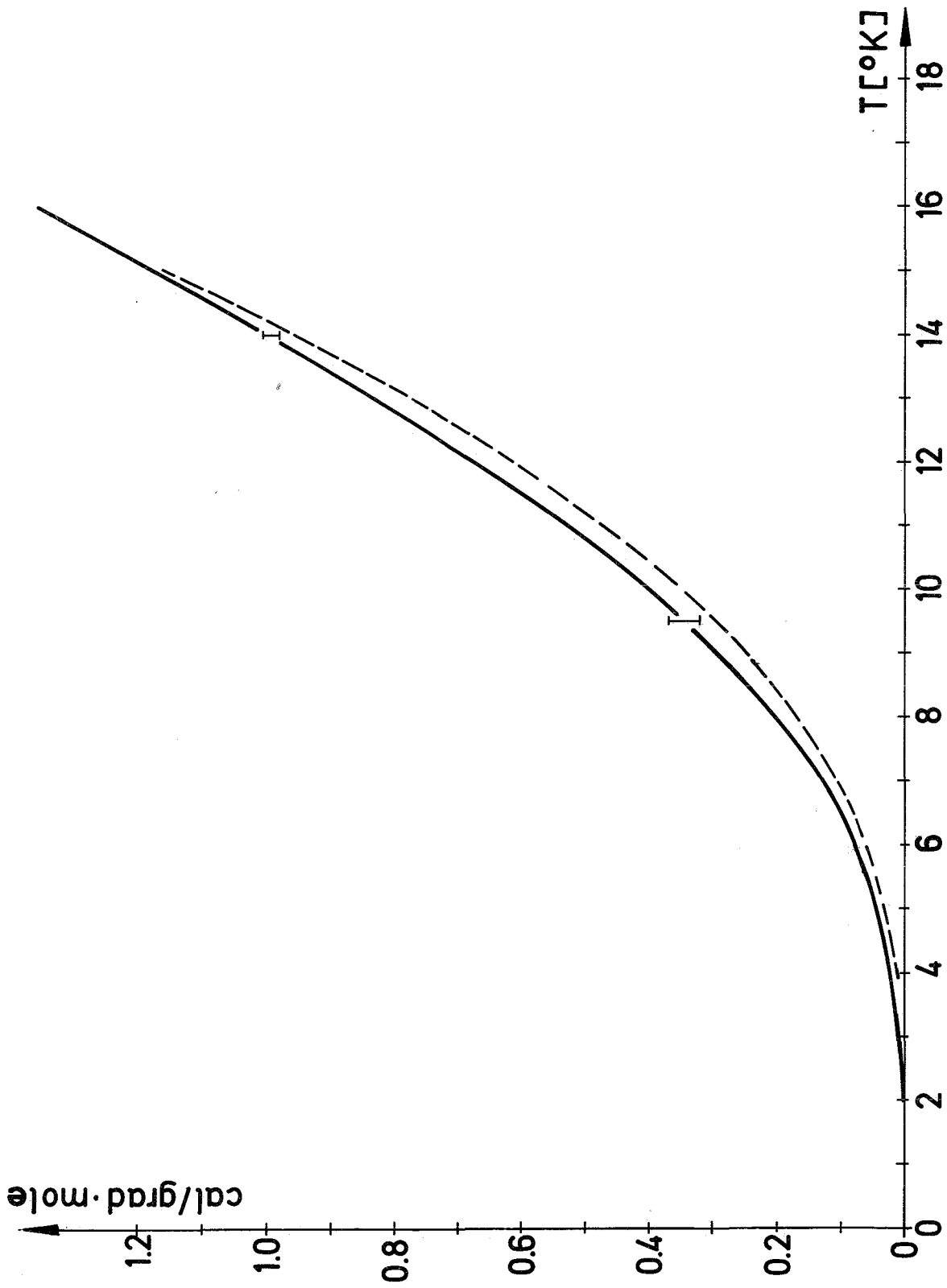
Specific Heat Cv(T) of Solid Hydrogen c=0.68

Fig.13